

# Sequential $^1\text{H}$ NMR Assignments of Iron(II) Cytochrome $c_{551}$ from *Pseudomonas aeruginosa*<sup>†</sup>

David J. Detlefsen,<sup>†</sup> V. Thanabal,<sup>§</sup> V. L. Pecoraro,<sup>‡</sup> and Gerhard Wagner<sup>\*,§</sup>

Department of Chemistry, The University of Michigan, Willard H. Dow Laboratory, Ann Arbor, Michigan 48109, and Institute of Science and Technology, Biophysics Research Division, The University of Michigan, 2200 Bonisteel Boulevard, Ann Arbor, Michigan 48109

Received May 21, 1990; Revised Manuscript Received July 12, 1990

**ABSTRACT:** Sequence-specific  $^1\text{H}$  NMR resonance assignments for all but the C-terminal Lys 82 are reported for iron(II) cytochrome  $c_{551}$  from *Pseudomonas aeruginosa* at 25 °C and pH = 6.8. Spin systems were identified by using TOCSY and DQF-COSY spectra in  $^2\text{H}_2\text{O}$  and  $^1\text{H}_2\text{O}$ . Sequential assignments were made by using NOESY connectivities between adjacent amide,  $\alpha$ , and  $\beta$  protons. Resonances from several amino acids including His 16, Gly 24, Ile 48, and Met 61 experience strong ring-current shifts due to their placement near the heme. All heme protons, including the previously unassigned propionates, have been identified. Preliminary analysis of sequential and medium-range NOEs provides evidence for substantial amounts of helix in the solution structure. Long-range NOEs indicate that the folds in solution and crystal structures are similar. For one aromatic side chain (Tyr 27) that is close to the heme group we found a transition from hindered ring rotation at low temperature to rapid rotation at high temperature.

A detailed description of the factors that regulate long-range electron transfer in biological systems is essential for a thorough understanding of energy production and utilization in every organism. Although extensive development in the theoretical treatment of biological electron transfer has occurred in the last 20 years (Marcus & Sutin, 1985), the fundamental nature of these reactions is still not fully understood. There is a clear dependence of the electron-transfer rate on distance (McLendon, 1988; Gray & Malmström, 1989); however, other factors such as electron transfer mediation by low-lying, empty  $\pi^*$  orbitals of side-chain aromatics or vacant 3d orbitals of sulfur may significantly alter the efficiency of the process. More recently, the idea of conformational gating as a primary regulator of long-range electron transfer has been proposed (McLendon et al., 1987; Hoffman & Ratner, 1987). It also appears that one must not only consider the static protein conformations but also the interactions between these macromolecules both before and after the electron-transfer event.

One protein that has been extensively studied is cytochrome  $c_{551}$  from *Pseudomonas aeruginosa*, which is believed to function in the terminal electron-transfer chain of this organism (Horio, 1958). The kinetics of electron transfer between cytochrome  $c_{551}$  and azurin, a blue copper protein also isolated from *P. aeruginosa*, have been extensively studied [for recent reviews, see Farver & Pecht, (1989, 1984)]. Complicating the kinetic analysis of this rapid electron transfer are conformational changes (Rosen & Pecht, 1976; Wilson et al., 1975) in both azurin and cytochrome  $c_{551}$ . On the basis of kinetic studies of chemically modified azurins, using Cr(III) labels, it has been proposed that the  $\pi$  orbitals of His 35 of azurin interact with the  $\pi$  orbitals of the cytochrome  $c_{551}$  heme to accomplish electron transfer (Farver & Pecht, 1989). The interaction between these proteins is weak (D. J. Detlefsen and

V. L. Pecoraro, manuscript in preparation, 1990).

Although the X-ray crystal structures of both the ferric and ferrous cytochrome  $c_{551}$  are known to 1.6-Å resolution (Matsuura et al., 1982), there is little data available to analyze solution structural characteristics. The reduced form of azurin has at least two conformations that appear to be related to the protonation state of His 35 (Mittra & Bersohn, 1982). The oxidized form of cytochrome  $c_{551}$  is also conformationally labile, although it is unknown whether pH affects this conversion. It is recognized, however, that the reduction potential is pH sensitive and is thought to be associated with a protein functional group (heme propionate) with  $\text{p}K_a \approx 7$  (Leitch et al., 1984).

*P. aeruginosa* cytochrome  $c_{551}$  is an ideal candidate for solution NMR<sup>1</sup> experiments. It consists of a single polypeptide chain of 82 amino acids and a c-type heme (Ambler, 1963) with a total molecular weight of 9200. Previous solution structural evaluation of *P. aeruginosa* cytochrome  $c_{551}$  consisted entirely of one-dimensional  $^1\text{H}$  NMR studies, resulting in assignment of most of the heme resonances and a few scattered amino acids [see, for example, Keller et al. (1976), Moore et al. (1977), Senn et al. (1980, 1984), and Leitch et al. (1984)], although, recently, the proton assignments of horse heart cytochrome *c* (a larger, structurally similar protein) for both Fe(II) and Fe(III) oxidation states have been reported (Wand et al., 1989; Feng et al., 1989). Herein we report the sequential assignment for protein and heme proton resonances of *P. aeruginosa* cytochrome  $c_{551}$  at 25 °C and pH 6.8 using 2D  $^1\text{H}$  NMR spectroscopy. The data described below provide the first step in defining the solution structure of the iron(II) cytochrome  $c_{551}$  at the low-pH side of the redox crucial  $\text{p}K_a$ . We are in the process of determining the solution structure by distance geometry calculations. The results will be published in a separate report.

<sup>†</sup> This study was supported by NSF (BBS-8615223), NIH (Grant 1GM38608), G. D. Searle/Chicago Community Trust to V.L.P., and the Institute for Protein Structure and Design and Research Partnership fellowships both from the University of Michigan to D.J.D.

\* Author to whom correspondence should be addressed.

<sup>‡</sup> Department of Chemistry, University of Michigan.

<sup>§</sup> Institute of Science and Technology, University of Michigan.

<sup>1</sup> Abbreviations: NMR, nuclear magnetic resonance; 2D, two-dimensional; ppm, parts per million; COSY, 2D correlated spectroscopy; TOCSY, total correlated spectroscopy; DQF-COSY, double quantum filtered COSY; NOE, nuclear Overhauser effect; NOESY, 2D NOE spectroscopy; Fe(II)  $c_{551}$ , iron(II) cytochrome  $c_{551}$ .

## MATERIALS AND METHODS

**Sample Preparation.** Ferrous cytochrome  $c_{551}$  was isolated from *P. aeruginosa* (PAO1) and purified by a procedure previously described (Horio, 1958; Parr et al., 1975; Wharton, 1975). Protein purity was verified as indicated by a single band on SDS-PAGE with silver stain. All NMR data were collected on 5 mM Fe(II)  $c_{551}$  in 50 mM potassium phosphate (pH = 6.8) unless otherwise noted. The following procedure was used to prepare freshly reduced Fe(II)  $c_{551}$  prior to each set of experiments. A 1 M solution of sodium dithionite in 50 mM potassium phosphate (pH = 6.8) was prepared and degassed with cycles of vacuum and argon. The protein sample was degassed by a similar process, in the NMR tube. A volume of the degassed 1 M dithionite (equivalent to 3-fold molar excess of the protein sample) was added with a Hamilton syringe and the reduced sample was degassed again. The NMR tube was sealed with a rubber septum and wrappings of Parafilm. Protein samples prepared in this manner remained reduced to greater than 99% for a period of up to 1 week. Spectra in  $^2\text{H}_2\text{O}$  were collected at two levels of exchange: level I exchange, where the protein was lyophilized from 50 mM potassium phosphate and dissolved in 99.99%  $^2\text{H}_2\text{O}$  and spectra were collected immediately, or level II exchange, where the partially exchanged sample was heated to 50 °C for 2 h, lyophilized, and redissolved in 99.99%  $^2\text{H}_2\text{O}$ . The heat-treated protein was judged intact since all  $^1\text{H}$  NMR resonances, other than those associated with exchangeable protons, remained unchanged. Seventeen amide protons remained after this treatment. Water samples contained 5%  $^2\text{H}_2\text{O}$  for a deuterium lock.

**NMR Spectroscopy.** All NMR data were collected on a General Electric GN-500 spectrometer and processed on Sun workstations using FT NMR (Hare Research, Inc). Spectra were collected in both 95%  $\text{H}_2\text{O}/5\%$   $^2\text{H}_2\text{O}$  and 99.99%  $^2\text{H}_2\text{O}$ . The solvent signal in 95%  $\text{H}_2\text{O}/5\%$   $^2\text{H}_2\text{O}$  was presaturated with low-power continuous-wave radiofrequency irradiation. Double quantum filtered COSY spectra (DQF-COSY) were obtained according to Piantini et al. (1982), Shaka and Freeman (1983), and Rance et al. (1984) with 1000  $t_1$  values and 2K complex  $t_2$  data points. 2D total correlation spectra [TOCSY as described by Braunschweiler and Ernst (1983) and Müller and Ernst (1979)] were collected at 15 and 25 °C by using an MLEV17 spin lock (Bax & Davis, 1985). TOCSY spectra were collected with several (four or more) mixing times with 700  $t_1$  values and 2K  $t_2$  data points and coadded to a single file to get complete spin system assignments. NOESY (Jeener et al., 1979; Kumar et al., 1980) spectra were recorded at 15 and 25 °C with mixing times varying from 75 to 200 ms collecting 740  $t_1$  values and 4K  $t_2$  data points. Two-dimensional data were multiplied by appropriately matched sine bell window functions in both  $\omega_1$  and  $\omega_2$ . All data were zero filled in  $\omega_1$  to 2K real data points. The TOCSY spectra were base-plane corrected by using a procedure of M. Adler and G. Wagner (manuscript in preparation, 1990). All spectra were collected by using the time proportional phase incrementation (TPPI) method for sign discrimination along  $\omega_1$  (Marion & Wüthrich, 1983). Chemical shifts were referenced with respect to  $\text{H}_2\text{O}$ , which in turn was calibrated by using internal 2,2-dimethyl-2-silapentane-5-sulfonate (DSS).

## RESULTS

*P. aeruginosa* cytochrome  $c_{551}$  contains 82 amino acids, which are divided among 36 unique (7 glycines, 13 alanines, 2 threonines, 7 valines, 4 leucines, and 3 isoleucines), 19 AMX<sup>2</sup>

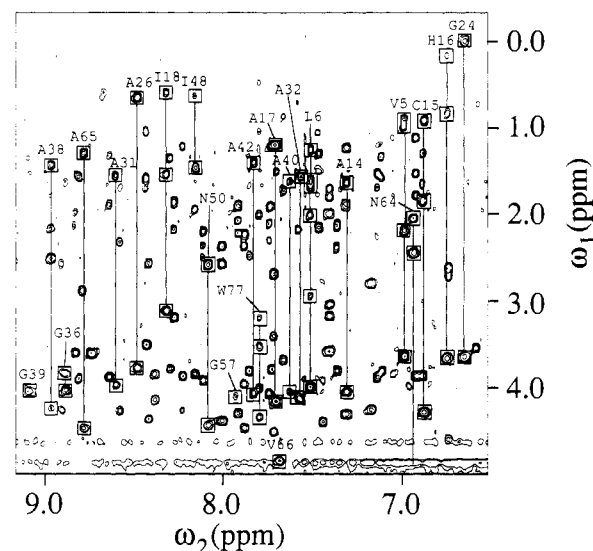


FIGURE 1:  $\text{H}_2\text{O}$  TOCSY spectra of iron(II) cytochrome  $c_{551}$  in 50 mM phosphate (pH = 6.8) at 25 °C. Four mixing times of 21.7, 30.5, 43.5, and 60.9 ms were coadded to give this spectrum. This region contains crosspeaks between amide protons and side-chain protons where unique and AMX spin systems are labeled. Vertical lines indicated common scalar coupling to an amide proton. Connected boxes indicate spins that belong to the same spin system. Sequential identities of amino acids are indicated at the top end (high field in  $\omega_1$ ) of the system.

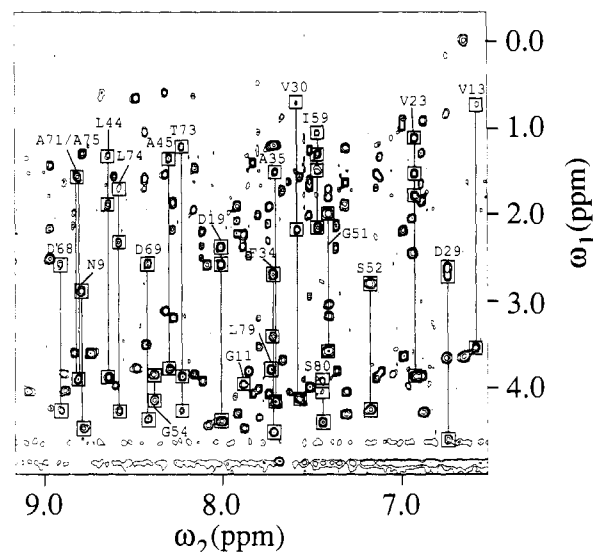


FIGURE 2: Same as Figure 1 for more unique and AMX spin systems.

(2 cysteines, 3 serines, 2 phenylalanines, 1 tyrosine, 2 tryptophans, 1 histidine, 5 aspartic acids, and 3 asparagines), and 27 long (2 methionines, 1 arginine, 8 lysines, 6 prolines, 5 glutamic acids, and 5 glutamines) spin systems. The assignments of spin systems to these types of residues are documented in Figures 1–3 (for 65 amino acids) where crosspeaks between backbone amide protons and  $\text{H}^\alpha$  or side-chain protons were observed in a TOCSY spectra collected in  $\text{H}_2\text{O}$ . Six residues (Asp 2, Thr 20, Val 55, Trp 57, Ser 67, and Val 78) were outside the spectral range of these figures. Portions of all six prolines are shown in Figure 4 with TOCSY connectivity from the  $\text{H}^\alpha$  proton. Five residues (Glu 1, Phe 7, Cys 12, Tyr 27, and Lys 82) did not show any TOCSY connectivity from the amide proton under the conditions described. Not all residues

<sup>2</sup> The term AMX spin systems is used for residues that form an AMX spin system in the absence of the amide proton (in  $^2\text{H}_2\text{O}$ ) to follow the usual nomenclature (Wüthrich, 1986).

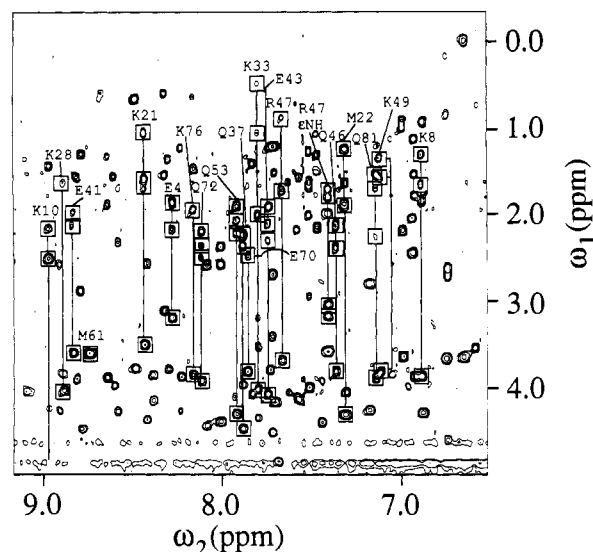
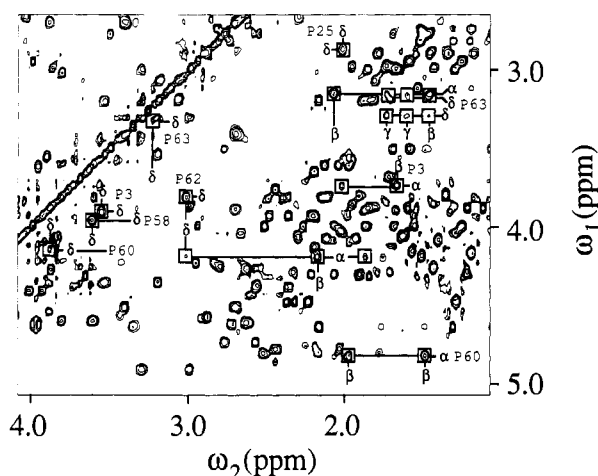


FIGURE 3: Same as Figure 1 for long spin systems.

FIGURE 4:  $^2\text{H}_2\text{O}$  TOCSY spectra of iron(II) cytochrome  $c_{551}$  in 50 mM phosphate (pH = 6.8) at 25 °C showing spin-system connectivities for prolines. Connected boxes indicate spins that belong to the same spin system. Sequential identities of amino acids are indicated next to the boxes.

showed TOCSY connectivities from the amide proton to all side-chain protons to afford an unambiguous assignment of the spin system. In these cases, other portions of TOCSY and DQF-COSY spectra were examined to verify the assignment. These data are mentioned without being shown to verify the assignment to a spin system type or as additional evidence. The assignment of Fe(II)  $c_{551}$  proceeded as follows: (i) identification of all of the unique spin systems, most of the AMX spin systems, and a few of the long spin systems; (ii) sequential assignment using backbone  $\text{H}^N$ ,  $\text{H}^\alpha$ , and  $\text{H}^\beta$  protons; and (iii) completion of spin system identification during sequential assignment process by referring the aliphatic portions of  $^2\text{H}_2\text{O}$  TOCSY or DQF-COSY (usually for long spin systems). The results are divided into six sections including (1) spin system, (2) side-chain amine and amide, (3) aromatic side chain, (4) heme group, (5) sequential, and (6) proline sequential assignments.

#### (1) Spin System Assignments

**Unique Spin Systems.** Figures 1 and 2 show TOCSY connectivities for all unique spin systems including glycines, alanines, valines, threonines, and leucines except for Thr 20, Val 55, and Val 78, which showed crosspeaks from the amide proton to all protons in the spin system in other portions of

the fingerprint region. All 13 alanines showed intrareidue connectivities to their complete spin system in Figures 1 and 2. Ala 71 and Ala 75 were difficult to distinguish, owing to the nearly complete degeneracy of all spins between the two. The ambiguity was resolved by examining the  $\alpha$  to  $\beta$  crosspeaks in a DQF-COSY for accurate  $\text{H}^\alpha$  and  $\beta\text{-CH}_3$  chemical shifts followed by careful analysis of the sequential connectivity patterns in the water NOESY spectra at 15 and 25 °C.

The seven glycines were identified in Figures 1 and 2. Gly 24, Gly 36, Gly 51, and Gly 54 all showed crosspeaks from the amide proton to both  $\alpha$  protons while Gly 11, Gly 39, and Gly 57 showed connectivity to only one  $\alpha$  proton. All glycines except Gly 36 showed well-resolved  $\alpha$  to  $\alpha$  crosspeaks in the DQF-COSY spectra with large coupling constants indicative of geminal protons. A two-quantum spectrum verified Gly 11, Gly 24, Gly 51, and Gly 57 as glycines on the basis of the appearance of two direct peaks and a remote peak at  $[\omega_2 = \text{NH}, \omega_1 = (\text{H}^{\alpha 1} + \text{H}^{\alpha 2})]$  (Wagner & Zuiderweg, 1983). Although a Gly 36  $\text{H}^\alpha$  to  $\text{H}^\alpha$  crosspeak was not clearly visible in either TOCSY or DQF-COSY spectra, this spin system was identified on the basis of TOCSY connectivities from an amide proton to two protons in the  $\alpha$ -proton chemical shift region of Figure 1 and verified as Gly 36 during the sequential assignment process (vide infra).

Thr 73 and Thr 20 showed coupling from the amide to  $\text{H}^\alpha$ ,  $\text{H}^\beta$ , and  $\gamma\text{-CH}_3$  resonances. Thr 73 is documented in Figure 2; Thr 20 is outside the spectral range (Table I).

Leu 6, Leu 44, and Leu 74 showed TOCSY crosspeaks from the amide proton to three or more spins in Figures 1 and 2. These were verified as leucines on the basis of analysis of both TOCSY and DQF-COSY spectra in the aliphatic region. Leu 79 was difficult to assign since TOCSY connectivity could not be traced past the  $\alpha$  proton from the amide in Figure 2. This leucine was assigned by tracing TOCSY (in a  $^2\text{H}_2\text{O}$  spectrum) connectivity in the aliphatic region back from the  $\text{H}^\gamma$  to the  $\text{H}^\beta$ s and subsequently connecting these  $\beta$  protons to the Leu 79  $\text{H}^\alpha$  by NOESY intrareidue connectivity.

All three isoleucines showed TOCSY crosspeaks from their amide protons to two or more spins as shown in Figures 1 and 2. The complete spin systems for Ile 18 and Ile 59 could be seen in TOCSY crosspeaks from their respective  $\alpha$  protons. Ile 48 was somewhat more difficult to assign owing to the unusual chemical shift of its  $\alpha$  proton (1.46 ppm); however, this spin system was assigned by tracing scalar connectivity in the TOCSY and DQF-COSY spectra in the aliphatic region.

The spin systems of all valines (except for Val 55 and Val 78) were identified in Figures 1 and 2. Val 5 and Val 23 showed TOCSY crosspeaks from the amide proton to the entire spin system while Val 13, Val 30, and Val 66 gave crosspeaks to portions of their systems. Val 55 and Val 78 showed complete TOCSY connectivity from the amide proton in a region downfield of the view of Figures 2 and 3.

**AMX Spin Systems.**<sup>2</sup> Fifteen of the 19 AMX spin systems showed TOCSY connectivities from the amide protons (13 are within the spectral range of Figures 1 and 2). Residues Cys 15, His 16, Asp 19, Asp 29, Phe 34, Trp 77, and Ser 80 all showed connectivities from the amide proton to the  $\text{H}^\alpha$  and both  $\text{H}^\beta$  protons. Two AMX spin systems did not show TOCSY connectivities to their  $\text{H}^\alpha$  protons (Asp 2 and Asp 64). TOCSY crosspeaks were noted for Asp 2 (downfield of Figures 1 and 2) from the amide to both  $\text{H}^\beta$  protons; the  $\text{H}^N$  to  $\text{H}^\alpha$  crosspeak could not be identified since the  $\alpha$  proton (4.73) is coincidental with the water line. A similar situation was observed for Asn 64 ( $\text{H}^\alpha = 4.78$  ppm) shown in Figure 1. AMX spin systems Asn 9, Asn 50, Ser 52, Asp 68, and

**Table 1:** Chemical Shifts for the Assigned Proton NMR Resonances of Iron(II)  $c_{551}$  from *P. aeruginosa* at 25 °C and pH = 6.8

residue	HN	H <sup>a</sup>	H <sup>b</sup>	others <sup>a</sup>
E1		3.99	2.08, 1.87	2.27 H <sup>γ</sup> , 2.52 H <sup>γ</sup>
D2	9.42	4.73	2.78, 2.57	
P3		3.74	1.67	1.58 H <sup>γ</sup> , 3.91 H <sup>δ</sup> , 3.55 H <sup>δ</sup> , 2.02, 0.78
E4	8.27	3.19	1.82, 1.87	2.19 H <sup>γ</sup>
V5	7.01	3.64	2.19	0.96 H <sup>γ</sup> , 0.88 H <sup>γ</sup>
L6	7.54	4.06	2.03, 1.25	1.59 H <sup>γ</sup> , 0.88 H <sup>δ</sup> , 0.87 H <sup>δ</sup>
F7	8.38	4.24	2.97, 2.86	7.26 H(2,6), 7.12 H(4), 6.91 H(3,5)
K8	6.89	3.87		1.83, 1.63, 1.27
N9	8.80	4.58	2.90, 2.90	7.67 H <sup>δ</sup> , 6.96 H <sup>δ</sup>
K10	8.97	4.80	2.53	1.42, 2.20
G11	7.88	4.62, 3.97		
C12	8.46	4.92	3.30, 3.00	
V13	6.61	3.53	0.98	0.81 H <sup>γ</sup> , 0.61 H <sup>γ</sup>
A14	7.32	4.07	1.62	
C15	6.87	4.30	1.79, 0.93	
H16	6.75	3.68	0.82, 0.13	0.66 H(2), 0.56 H(4)
A17	7.72	4.16	1.18	
I18	8.34	3.14	1.50	1.22 H <sup>γ1</sup> , 0.68 H <sup>γ1</sup> , 0.52 H <sup>γ2</sup> , 0.59 H <sup>δ</sup>
D19	8.03	4.41	2.61, 2.40	
T20	6.46	4.34	3.70	0.89 H <sup>γ</sup>
K21	8.43	3.51	1.71, 1.60	2.55, 1.02
M22	7.31	4.28		1.82, 1.90, 1.53, 1.20
V23	6.92	3.87	1.79	1.53 H <sup>γ</sup> , 1.10 H <sup>γ</sup>
G24	6.67	3.64, -0.03		
P25		3.50	0.86, 0.42	0.12 H <sup>γ</sup> , 0.02 H <sup>γ</sup> , 2.86 H <sup>δ</sup> , 2.01 H <sup>δ</sup>
A26	8.50	3.76	0.69	
Y27	7.52	4.04	2.66, 2.28	5.71 H(2,6), 4.58 H(3,5) <sup>b</sup>
K28	8.88	4.04	1.62	
D29	6.62	4.67	2.75, 2.67	
V30	7.61	4.12	2.18	1.55 H <sup>γ</sup> , 0.69 H <sup>γ</sup>
A31	8.63	3.98	1.54	
A32	7.59	4.15	1.55	
K33	7.84	4.02	1.99	1.17, 0.46, 1.05
F34	7.69	4.52	3.41, 2.69	7.62 H(2,6), 7.65 H(3,5), 7.6 H(4)
A35	7.71	4.18	1.50	
G36	8.89	4.02, 3.93		
Q37	7.73	4.50	2.20	2.32 H <sup>γ</sup> , 2.34 H <sup>γ</sup> , 6.81 H <sup>ε</sup> , 7.63 H <sup>ε</sup>
A38	8.97	4.25	1.41	
G39	9.10	4.06, 3.83		
A40	7.70	4.05	1.60	
E41	8.82	3.60	1.98	2.14, 2.87, 2.07
A42	7.86	4.07	1.38	
E43	7.77	4.08	2.10, 1.92	2.30
L44	8.66	3.88	1.87, 1.33	1.65 H <sup>γ</sup> , 0.78 H <sup>δ</sup> , 0.75 H <sup>δ</sup>
A45	8.32	3.78	1.34	
Q46	7.38	3.82	2.14	2.38 H <sup>γ</sup> , 7.01 H <sup>ε</sup> , 7.29 H <sup>ε</sup>
R47	7.68	3.66	1.72	3.18 H <sup>δ</sup> , 3.05 H <sup>δ</sup> , 7.43 H <sup>ε</sup> , 6.49 H <sup>γ</sup> , 1.80, 0.89
I48	8.15	1.46	1.70	0.62 H <sup>γ2</sup> , 1.28 H <sup>δ</sup>
K49	7.11	3.82	1.35, 1.56	
N50	8.08	4.44	2.56, 2.56	7.01 H <sup>δ</sup> , 7.30 H <sup>δ</sup>
G51	7.39	3.56, 1.97		
S52	7.18	4.28	2.78, 2.78	
Q53	7.91	4.28	1.90	2.22 H <sup>γ</sup> , 2.06 H <sup>γ</sup> , 6.84 H <sup>ε</sup> , 7.47 H <sup>ε</sup>
G54	8.42	4.14, 3.85		
V55	10.45	3.75	2.43	1.01 H <sup>γ</sup> , 0.64 H <sup>γ</sup>
W56	10.73	4.62	3.84, 3.61	11.57 HN side, 7.70 H(2), 8.03 H(4), 7.28 H(5), 7.10 H(6), 7.59 H(7)
G57	7.93	4.56, 4.11		
P58				3.96 H <sup>δ</sup> , 3.62 H <sup>δ</sup>
I59	7.45	4.64	2.16	1.76 H <sup>γ1</sup> , 1.48 H <sup>γ1</sup> , 1.30 H <sup>γ2</sup> , 1.05 H <sup>δ</sup>
P60		4.82	1.98, 1.49	3.92 H <sup>δ</sup> , 4.09 H <sup>δ</sup>
M61	8.77	3.62	-0.89, -2.72	-0.54 H <sup>γ</sup> , -3.55 H <sup>γ</sup> , -2.96 H <sup>ε</sup>
P62		4.19	2.17	3.81 H <sup>δ</sup> , 3.02 H <sup>δ</sup>
P63		3.14	1.45, 2.07	1.72 H <sup>γ</sup> , 1.60 H <sup>γ</sup> , 3.18 H <sup>δ</sup> , 3.27 H <sup>δ</sup>
N64	6.92	4.78	2.02, 2.43	
A65	8.83	4.47	1.28	
V66	7.70	4.84	2.44	0.71 H <sup>γ</sup> , 0.58 H <sup>γ</sup>
S67	9.24	4.55	3.88, 4.35	
D68	8.81	4.28	2.54, 2.59	
D69	8.42	4.36	2.55, 2.55	
E70	7.85	3.82	2.47	
A71	8.82	3.92	1.55	
Q72	8.11	3.93	2.20, 2.20	2.36 H <sup>γ</sup> , 2.47 H <sup>γ</sup> , 6.64 H <sup>ε</sup> , 7.70 H <sup>ε</sup>
T73	8.23	3.97	4.29	1.23 H <sup>γ</sup>
L74	8.59	4.28	2.33, 1.71	1.78 H <sup>γ</sup> , 1.18 H <sup>δ</sup> , 1.18 H <sup>δ</sup>
A75	8.81	3.87	1.58	
K76	8.19	3.87	1.96	1.43
W77	7.80	4.37	3.53, 3.21	10.18 HN side, 7.24 H(2), 7.34 H(4), 6.39 H(5), 5.77 H(6), 7.07 H(7)

Table I (Continued)

residue	HN	H <sup>α</sup>	H <sup>β</sup>	others <sup>a</sup>			
V78	9.18	2.54	2.18	0.61 H <sup>γ</sup> , 0.42 H <sup>γ</sup>			
L79	7.75	3.81	1.90, 1.55	1.81 H <sup>γ</sup> , 0.88 H <sup>δ</sup> , 0.82 H <sup>δ</sup>			
S80	7.44	4.41	4.02, 3.93				
Q81	7.15	3.89	2.28	1.72, 1.53			
K82							
heme assignments <sup>c</sup>		heme assignments <sup>c</sup>		heme assignments <sup>c</sup>		heme assignments <sup>c</sup>	
α meso	9.80	4-H	6.11	5-methyl	3.26	6-prop (6L1)	4.22, 4.57
β meso	9.31	2-H	5.87	8-methyl	3.35	6-prop (6L2)	2.63, 3.41
γ meso	9.28	3-methyl	3.70	4-methyl	2.37	7-prop (7L1)	3.88, 4.62
δ meso	9.18	1-methyl	3.64	2-methyl	1.79	7-prop (7L2)	2.69, 3.34

<sup>a</sup> Resonances in "others" column that are not labeled are known to belong to the spin system but the exact assignment to a position in the side chain was not made. Heme resonances are listed at the end of the table. <sup>b</sup> Tyr 27 (3,5) chemical shift at 60 °C; see the Results section for a discussion. <sup>c</sup> IUPAC/IUB nomenclature used for heme propionates indicated parenthetically.

Asp 69 showed TOCSY connectivities from the amide to the H $^{\alpha}$  and only one H $^{\beta}$  due to degeneracy in the  $\beta$ -proton chemical shifts. Three sets of  $\beta$  protons (Asn 9, Asn 50, and Asp 69) were confirmed to be degenerate by the identification of a remote crosspeak ( $\omega_2 = \text{H}^{\alpha}$ ,  $\omega_1 = \text{H}^{\beta} + \text{H}^{\beta}$ ) (Wagner & Zuiderweg, 1983) in the two-quantum spectrum. The  $\beta$  protons of Ser 67 showed no connectivity from their amide proton outside the spectral range of these figures (the amide to H $^{\alpha}$  crosspeak for Ser 67 was observed in the DQF-COSY and 15 °C TOCSY).

Four AMX spin systems showed no TOCSY connectivity with their amide protons (Phe 7, Cys 12, Tyr 27, and Trp 56). Phe 7 was initially identified in DQF-COSY and TOCSY spectra as an AMX spin system with the H $^{\alpha}$  proton at 4.24 ppm. Sequential connectivities from Leu 6 ( $d_{\alpha\text{N}}$  and  $d_{\text{NN}}$ ) and Lys 8 ( $d_{\text{NN}}$  and  $d_{\beta\text{N}}$ ) as well as intraresidue NOEs from the H $^{\beta}$  protons to the (2,6) ring protons of a phenylalanine aromatic moiety served to confirm this assignment. The Cys 12 amide resonance was identified during the sequential assignment process, showing strong intraresidue NOEs to H $^{\beta}$ s of an unassigned AMX spin system. Tyr 27 proved to be difficult owing not only to the lack of TOCSY peaks from the amide proton but also as a result of difficulty in identifying its aromatic resonances (vide infra). Tyr 27 was assigned to an AMX spin system, verified in DQF-COSY and TOCSY spectra, with an H $^{\alpha}$  proton at 4.04 ppm. Sequential NOESY connectivities from Ala 26 ( $d_{\alpha\text{N}}$  and weak  $d_{\text{NN}}$ ) and Lys 28 ( $d_{\text{NN}}$ ) served to link the Tyr 27 H $^{\alpha}$  proton to its amide and place it sequentially. TOCSY crosspeaks were not observed from the amide of Trp 56, most likely because the MLEV17 spin lock was not effective near the edge of the spectrum; however, a DQF-COSY crosspeak was observed between the Trp 56 amide proton and H $^{\alpha}$  of this spin system and the spin system was well constrained by sequential NOEs (Figure 10).

**Long Spin Systems.** This cytochrome contains 27 amino acids with long spin systems, six of which are prolines. Met 22 showed connectivities from the amide to the H $^{\alpha}$  and two other intraresidue spins in the 25 °C TOCSY spectrum of Figure 3 (crosspeaks to all H $^{\beta}$ s and H $^{\gamma}$ s were seen in a 15 °C TOCSY spectrum). The side-chain resonances of Met 61 were located upfield of 0 ppm, presumably, owing to their location above the heme plane as an iron axial ligand. The resonances of Met 61 were assigned with a combination of DQF-COSY and two-quantum spectra. The H $^{\alpha}$  and amide protons were assigned on the basis of sequential NOEs to neighboring residues. The  $\beta$  proton at -0.89 ppm was assigned from a DQF-COSY crosspeak and subsequently verified by the observance of direct ( $\omega_2 = \text{H}^{\alpha}$ ,  $\omega_1 = \text{H}^{\alpha} + \text{H}^{\beta}$ ) and remote ( $\omega_2 = \text{H}^{\alpha}$ ,  $\omega_1 = \text{H}^{\beta} + \text{NH}$ ) two-quantum crosspeaks. The other

H $^{\beta}$  at -2.72 was identified on the basis of two two-quantum peaks ( $\omega_2 = \text{H}^{\alpha}$ ,  $\omega_1 = \text{H}^{\alpha} + \text{H}^{\beta}$ ;  $\omega_2 = \text{H}^{\beta}$ ,  $\omega_1 = \text{H}^{\alpha} + \text{H}^{\beta}$ ). The  $\epsilon$ -CH $_3$  was assigned to -2.96 since it is a singlet and showed NOESY crosspeaks to the rest of the Met 61 spin system but no scalar connectivity to the spins. This left the  $\gamma$  protons to be at -0.54 and -3.55 ppm.

The lysines, glutamic acids, glutamines, and arginines were assigned as follows. The Arg 47 backbone amide and side-chain amine protons are labeled in Figure 3. TOCSY crosspeaks can be seen from the amide proton to the H $^{\alpha}$  and one H $^{\beta}$ , and from the N $^{\epsilon}$ H proton to the H $^{\delta}$ s and H $^{\gamma}$ s. Furthermore, TOCSY crosspeaks were observed in  $^2\text{H}_2\text{O}$  between the H $^{\alpha}$  and both H $^{\delta}$ s. Portions of the spin systems of seven lysines can be seen in Figure 3 (Lys 82 NH proton was not identified). Lys 28, Lys 49, and Lys 76 each showed connectivity to only one other spin in addition to the  $\alpha$  proton while Lys 8, Lys 21, Lys 33, and Lys 49 showed crosspeaks with an additional two spins. All glutamate amide protons (except Glu 1 and Glu 70) gave TOCSY crosspeaks to at least two of their side-chain spins. The H $^{\alpha}$  and both H $^{\delta}$ s of Glu 1 were identified by a strong NOE from the Asp 2 amide proton. The remaining resonances for Glu 1 were assigned on the basis of analysis of  $^2\text{H}_2\text{O}$  TOCSY spectra in the aliphatic region. Five long spin systems in Figure 3 were identified as glutamines with each showing TOCSY connectivity to two or more side-chain spins in addition to the  $\alpha$  proton; four of these were verified as glutamines by showing NOESY connectivities to unassigned side-chain amide protons as discussed in the next section. The  $\beta$  protons of Gln 72 were degenerate as indicated by the appearance of a two-quantum remote peak ( $\omega_2 = \text{H}^{\alpha}$ ,  $\omega_1 = \text{H}^{\beta 1} + \text{H}^{\beta 2}$ ).

There are six prolines in cytochrome  $c_{551}$ . Figure 4 shows a portion of the  $^2\text{H}_2\text{O}$  TOCSY spectrum where these spin systems are documented. The complete spin system assignments were made for Pro 25 and Pro 63. Only the H $^{\delta}$  to H $^{\delta}$  crosspeak is shown for Pro 25, as the rest of the crosspeaks lie upfield in  $\omega_2$  of this view, whereas all assigned resonance for Pro 63 are shown. Pro 25 was easily assigned as a long spin system since many of its resonances fell in an empty region of the spectrum and no amide to H $^{\alpha}$  crosspeak could be found in TOCSY or DQF-COSY spectra. TOCSY crosspeaks for portions of Pro 62 are also shown in Figure 4, demonstrating the H $^{\alpha}$ , one H $^{\beta}$ , and both H $^{\delta}$ s. Pro 3, Pro 58, Pro 60, and Pro 62 will be discussed in more detail in the proline sequential assignment section.

## (2) Side-Chain Amine and Amide Assignments

The H $^{\epsilon}$  side-chain resonance of Arg 47 was identified on the basis of scalar coupling with the  $\delta$  protons shown in Figure

3. An amine proton belonging to the H<sup>γ</sup> Arg 47 side chain were identified by NOESY crosspeaks to the δ protons located in another region of the spectrum. The ring amine resonances for both Trp 56 and Trp 77 were assigned on the basis of a TOCSY crosspeak to the 2-proton of their respective spin system. The side-chain amides (H<sup>β</sup>s) of Asn 9 and Asn 50 gave NOESY crosspeaks to their respective β protons while Gln 37, Gln 46, Gln 53, and Gln 72 side-chain amide protons (H<sup>γ</sup>s) gave NOESY crosspeaks to at least one of their γ protons.

### (3) Aromatic Side-Chain Assignments

The 4-7-protons of both Trp 56 and Trp 77 were identified by examination of the crosspeak multiplet structure where the 4- and 7-protons are doublets with a 10-Hz splitting in the DQF-COSY while the 5- and 6-protons are triplets and show a 14-Hz separation of the outer multiplet components. Although the multiplet structure was not completely resolved, peaks consistent with this coupling analysis were assigned to the respective tryptophan side-chain protons. The assignment of the tryptophan aromatic resonances were confirmed by observance of the side-chain amine to 7-proton NOESY crosspeak in each case. The Trp 56 2-proton and Trp 77 2-proton were identified by DQF-COSY and TOCSY crosspeaks to the side-chain amine protons as well as NOESY crosspeaks to the H<sup>α</sup> and H<sup>β</sup>s.

Phe 7 ring protons were assigned on the basis of the identification of three sets of resonances with the (3,5) degenerate pair identified by scalar coupling to two resonances at 7.12 and 7.26 ppm. The latter resonance was assigned to the (2,6) pair on the basis of NOESY crosspeaks with the Phe 7 β protons. Phe 34 ring protons were initially assigned to an unresolvable cluster of resonances at approximately 7.6 ppm. Examination of the 25 °C NOESY data allowed for the tentative assignment of the 7.62 ppm resonance to the 2,6-protons and 7.65 the 3,5-protons since the former showed qualitatively stronger NOE interaction with the Phe 34 H<sup>β</sup>s. Since the 2,6-protons and the 3,5-protons are strongly coupled, the wave functions of both nuclei are mixed, and NOEs to the H<sup>β</sup>s can be expected for both aromatic resonances even though the distance between the H<sup>β</sup>s and the 3,5-protons is too large for a direct NOE. We indeed observed this NOE in a 100-ms NOESY, and it may not be due to spin diffusion (Keeler & Neuhaus; 1987). The Phe 34 4-proton was believed also to be at or near 7.6 ppm, consistent with the lack of scalar crosspeaks to the 7.65 and 7.62 ppm resonances.

The aromatic resonances of Tyr 27 were difficult to assign. Strong NOESY crosspeaks between Tyr 27 H<sup>α</sup> and H<sup>β</sup> protons indicated that the ring 2,6-protons might be located at 5.71 ppm. However, all attempts to find TOCSY or DQF-COSY connectivity to any other resonance failed at 5, 15, and 25 °C. It was not until a TOCSY spectrum at 60 °C was recorded that the Tyr 27 3,5-protons were identified at 4.58 ppm. The fact that we did not observe DQF-COSY or TOCSY crosspeaks to the 3,5-protons at lower temperatures suggests that these protons are broadened due to rotational motion as has been observed previously in other proteins (Wüthrich & Wagner; 1978), where, in a certain temperature range, the 3,5-protons are invisible while the 2,6-protons show the averaged signal of a rapidly rotating side chain.

### (4) Heme Group Assignments

Figure 5 contains diagrams showing two orientations of the heme group of c<sub>551</sub>. The double-headed arrows indicate the crucial observed NOEs involved in assigning all of the heme resonances by a procedure described by Keller and Wüthrich (1978). The process began with the identification of a meso

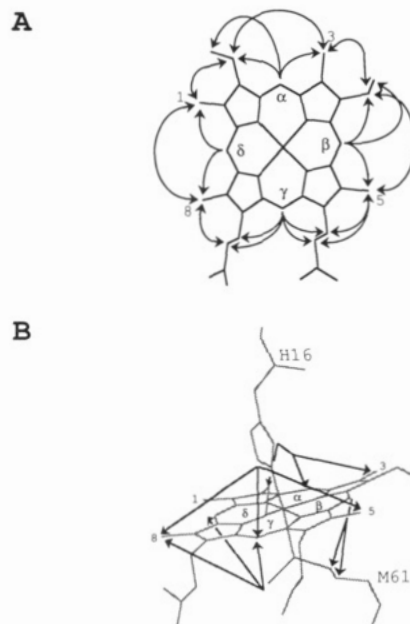


FIGURE 5: (A) Schematic of c-type heme group of cytochrome c<sub>551</sub> showing NOESY connectivities observed within the heme moiety. Arrows indicate NOE connectivities observed between heme resonances and axial ligands. (B) Another view of the c-type heme showing the axial ligands His 16 and Met 61 with the straight lines indicating the NOEs observed. The figure was constructed from X-ray crystal structure coordinates (Matsuura et al., 1982).

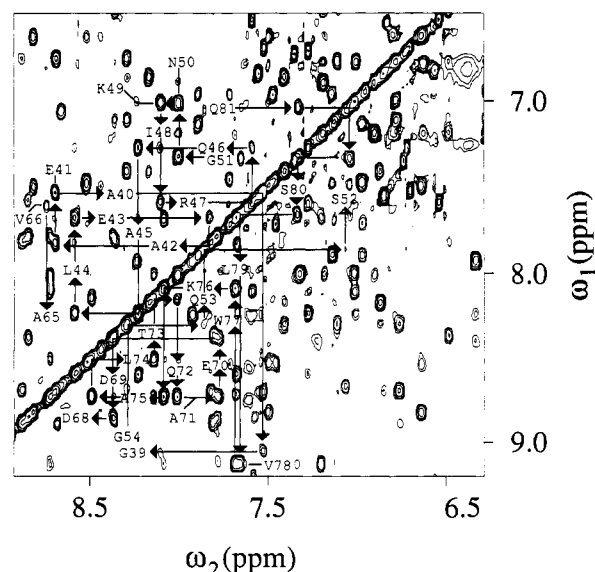
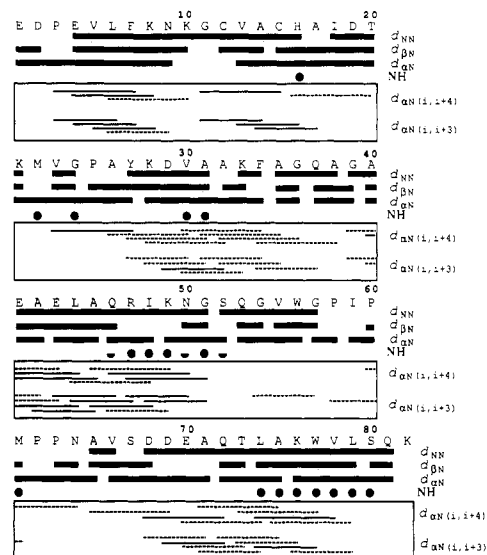
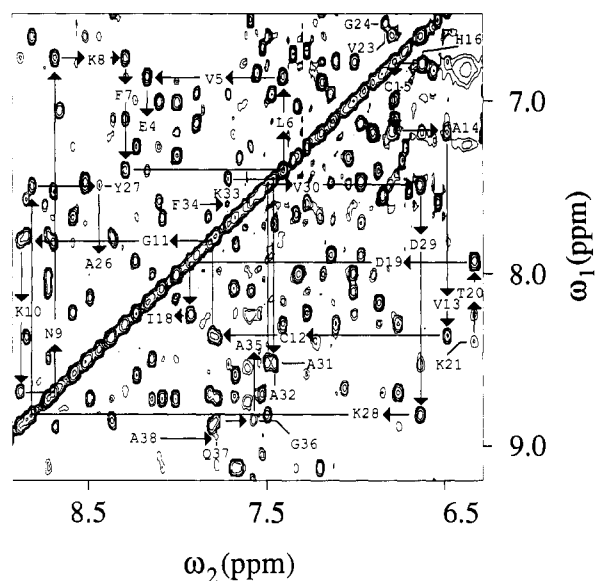
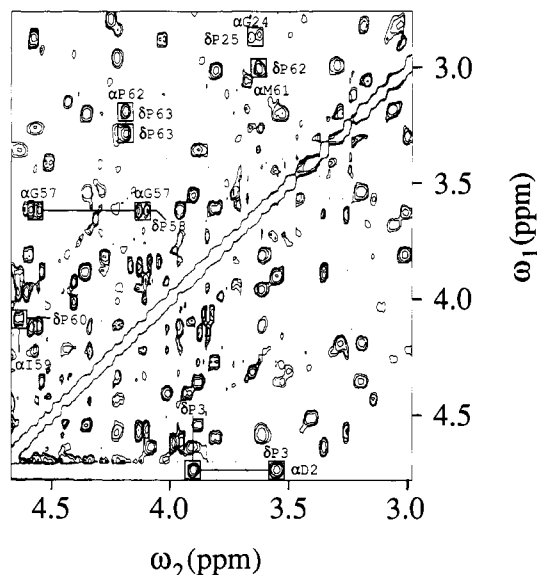
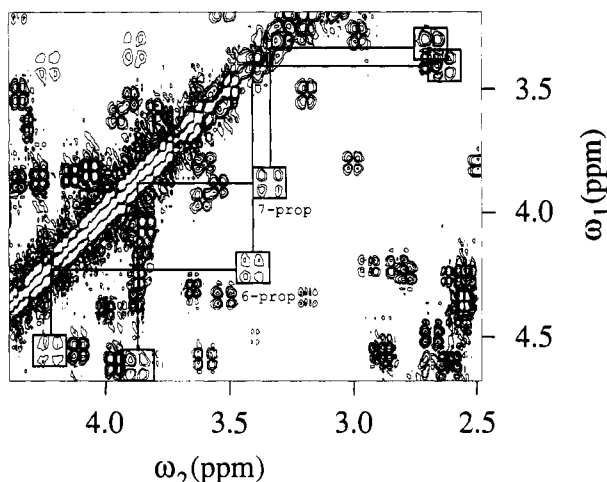
proton that showed NOESY crosspeaks to two methyls (δ meso to 1- and 8-methyls in Figure 5A). The 1- and 8-methyls were assigned on the basis of the 1-methyl showing an NOESY crosspeak to the 2-methyl as well as the 2-H resonance, while the 8-methyl gave NOESY crosspeaks to portions of the position 7 propionate. The rest of the heme assignments were verified with NOEs using these three positions for orientation and continuing around the heme periphery until the ends met. Figure 5B shows NOESY crosspeaks observed from axial ligands His 16 and Met 61 to heme resonances.

To our knowledge, this is the first time all propionate resonances have been assigned for an Fe(II) c-type cytochrome although the propionates have been assigned for Fe(III) horse heart cytochrome c (Feng et al., 1990), and portions of the propionates for Fe(II) c-type cytochromes (Santos & Turner, 1987; Yu & Smith, 1990). The initial clue consisted of two unassigned (four-spin) spin systems in the DQF-COSY that had no sequential NOESY assignment that were left over at the end of the assignment process. The coupling constants observed in the DQF-COSY peaks were large (similar to geminal glycine H<sup>α</sup>s). TOCSY provided the overall connectivity information. NOEs to heme methyls and the γ meso confirmed the propionate assignments. Figure 6 shows the DQF-COSY connectivities for the heme propionate side chains.

### (5) Sequential Assignments

The process of spin system and sequential assignments were not separated in this study. Often times, clear sequential NOEs provided information on spin system identity simply by placement of an amide to H<sup>α</sup> crosspeak in the midst of a unique stretch of amino acids. This was particularly true of long spin systems. A general procedure (Wagner et al., 1981; Wüthrich et al., 1982; Billeter et al., 1982; Wagner & Wüthrich, 1982) was followed for all sequential assignments. Connectivities for prolines are discussed separately since their placement is more difficult and involves a slightly different strategy. When a proline is encountered during this section,





its presence will simply be noted. Figures 7 and 8 show amide to amide proton sequential connectivities ( $d_{NN}$ ) in a NOESY spectrum (150 ms) collected at 15 °C. Further sequential connectivity in terms of  $d_{\alpha N}$  and  $d_{\beta N}$  are mentioned in support of the assignments. Sequential connectivities were established for all but three peptide links. These are between Phe 34 and Ala 35, between Pro 58 and Ile 59, and between Gln 81 and Lys 82. The sequential connectivities between Phe 34 to Ala 35 could not be established unambiguously since the amide protons of both residues and the ring protons of Phe 34 fall within a 0.2 ppm range. The sequential connectivities from Pro 58 to Ile 59 and Gln 81 to Lys 82 could not be made

because of incomplete spin system assignments of Pro 58 and Lys 82. The sequential assignment results are summarized in Figure 10.

Figure 7 shows  $d_{NN}$  connectivities from Glu 4 through His 16 and from Ile 18 through Lys 21. Although Ala 17 does not show sequential  $d_{NN}$  connectivity, it does have strong  $d_{\alpha N}$  and  $d_{\beta N}$  connectivities to Ile 18 in addition to  $d_{\alpha N}$  and  $d_{\beta N}$  from His 16. The  $d_{\alpha N}$  connectivities from Glu 4 through Lys 10 and Val 13 through Asp 19 have been noted in another portion of the NOESY spectrum. Gly 11 was difficult to assign sequentially. The difficulty arose in showing  $d_{\alpha N}$  connectivity to residues adjacent to Gly 11: the  $d_{\alpha N}$  for Lys 10 to Gly 11 was not visible since the Lys 10  $\alpha$  proton was near water (4.80 ppm) and no  $d_{\alpha N}$  for Gly 11 to Cys 12 could be found. The major elements of data that were used for placing it sequentially are as follows: Gly 11 was unambiguously assigned as a glycine spin system on the basis of two-quantum and  $^2\text{H}_2\text{O}$  TOCSY data as discussed previously and the Gly 11 amide shows a strong  $d_{NN}$  connectivity to Lys 10 and Cys 12 in Figure 7.

Figure 7 also documents the  $d_{NN}$  connectivity for Val 23 to Gly 24, Ala 26 to Phe 34, and Ala 35 through Ala 38. Interactions between Phe 34 to Ala 35 were unresolvable, as it was impossible to distinguish sequential NOEs ( $d_{\alpha N}$  Phe 34, Ala 35) from intrasidue NOEs from the Phe 34 phenyl group at 15 and 25 °C. Connectivity from Ala 38 to Gly 39 was demonstrated by the  $d_{\alpha N}$  and  $d_{\beta N}$  crosspeaks identified in another portion of the spectrum. In addition, the  $d_{\alpha N}$  interactions for Thr 20 through Tyr 27, Lys 28 to Phe 34, Ala 35 to Gly 36, and Gln 37 to Gly 39 were also noted. The  $d_{\alpha N}$  interaction for Tyr 27 to Lys 28 and was obscured due to degeneracy of the  $\alpha$ -proton chemical shifts. The assignment of Pro 25 is discussed in a later section.

The  $d_{NN}$  connectivities from Gly 39 to Gly 51, Ser 52 to Gly 54, and Ala 65 to Val 66 are shown in Figure 8. Similar  $d_{NN}$  interactions were observed for Val 55 through Gly 57 in another portion of the NOESY spectrum. The  $d_{\alpha N}$  connectivities for Ala 40 to Ala 42, Glu 43 through Ala 45, Gln 46 to Ile 48, Lys 49 to Ser 52, and Gln 53 to Trp 56 have been noted in another portion of the NOESY spectrum. The  $d_{\alpha N}$  connectivity of Ala 42 to Glu 43, Ala 45 to Gln 46, and Ser 52 to Gln 53 could not be seen, possibly due to overlap of  $\alpha$ -proton chemical shifts. The sequential assignment of Pro 58 is discussed later.

The stretch of amino acids from Pro 58 through Gln 81 proved challenging since it contains a sequence where four of six residues (Pro 58 to Pro 63) are prolines. This is a unique sequence resembling a collagen polyproline helix that is usually not observed in globular proteins (Richardson, 1981). The sequence of Pro 58 through Asn 64 will be discussed in the following section. Figure 8 shows the  $d_{NN}$  interactions for Asp 68 to Gln 81. The  $d_{NN}$  NOE for Asn 64 to Ala 65 interaction is weak but observable when the data are examined with a lower peak threshold value. The  $d_{NN}$  assignments of Asn 64 to Asp 68 are supported by NOESY crosspeaks in other portions of the spectrum. The Ala 65 to Val 66  $d_{\alpha N}$  was distinguished from the strong amide to  $\text{H}^\alpha$  interresidue NOE of Phe 34.

#### (6) Proline Sequential Assignments

It was anticipated that the assignment of residues Pro 58 to Pro 63 would be difficult owing to the abundance of proline residues. This difficulty was eased by the location of Met 61 in the midst of the polyproline helix and the clear spin-system identification of Pro 63. Starting from these two points, it was possible to make sequential assignments for this section and

identify major portions of the proline spin systems involved. Inspection of the  $^2\text{H}_2\text{O}$  NOESY data in the aliphatic region gave clues to where portions of proline spin systems might be located ( $\text{H}^\alpha$  to  $\text{H}^\delta$  sequential NOEs between the  $\text{H}^\alpha$  of the preceding amino acid and  $\text{H}^\delta$ s of the subsequent proline). Examination of the TOCSY spectra validated these as candidates for proline with the appearance of  $\text{H}^\delta$  to  $\text{H}^\delta$  crosspeaks. Sequential connectivity on the C-terminal end of prolines could be demonstrated by  $d_{\alpha N}$  connectivity. Once  $\text{H}^\alpha$  and  $\text{H}^\delta$ s were identified, the  $^2\text{H}_2\text{O}$  TOCSY spectrum was examined for evidence of scalar connectivity between these spins. Prolines were assigned by using this combination of NOESY and TOCSY spectra and this section details the combined analysis approach for the polyproline helical portion of  $c_{551}$ . This method worked in identifying Pro 62. The assignment of Pro 3 and Pro 58 could not be closed between the  $\text{H}^\alpha$  and  $\text{H}^\delta$  ends with scalar connectivity between spins identified as  $\text{H}^\alpha$  and  $\text{H}^\delta$ s during the sequential assignment process ( $\text{H}^\alpha$  to  $\text{H}^\delta$  crosspeaks were not observed).

Strong sequential  $\text{H}^\alpha$  to  $\text{H}^\delta$  NOEs were seen in Figure 9 for the Asp 2 to Pro 3 connectivity. Examination of the TOCSY spectrum at low plotting levels showed crosspeaks from the  $\text{H}^\alpha$  of Pro 3 to four other spins (two are shown in Figure 4). A weak sequential  $d_{\alpha N}$  crosspeak was observed for Pro 3 to Glu 4. The assignments of Pro 58 and Pro 60 remain incomplete. The  $\text{H}^\delta$ s of both were assigned on the basis of NOEs from the  $\alpha$  protons of the preceding residue (Figure 9), which led to  $\text{H}^\delta$  to  $\text{H}^\delta$  TOCSY crosspeaks. An  $\alpha$  proton could not be assigned to Pro 58. The Met 61 amide resonance gave strong  $d_{\alpha N}$  and  $d_{\beta N}$  crosspeaks to Pro 60 in another portion of the spectrum. Figure 9 shows the well-resolved  $\text{H}^\alpha$  to  $\text{H}^\delta$  sequential NOESY crosspeak demonstrating Pro 62 to Pro 63 connectivity. Pro 25 and Pro 63 had been identified as long spin systems prior to the sequential assignment process. Pro 25 was placed sequentially with strong  $\text{H}^\alpha$  to  $\text{H}^\delta$  NOESY crosspeaks to Gly 24 and  $d_{\alpha N}$  connectivity to Ala 26 noted in other portions of the NOESY spectrum. Figure 9 shows weak NOESY connectivity of Gly 24  $\text{H}^\alpha$  to Pro 25  $\text{H}^\delta$ . A strong  $d_{\alpha N}$  crosspeak was seen for Pro 63 to Asn 64 as well as a weak  $d_{\beta N}$  connectivity.

#### DISCUSSION

We have obtained an almost complete set of proton assignments for Fe(II)  $c_{551}$  from *P. aeruginosa*. Table I contains a listing of the chemical shift assignments for these as well as labile amide and side-chain amine protons. Sequential assignments of the backbone protons have been made for all but the terminal lysine residue (Lys 82) and the  $\alpha$ -proton of Pro 58 (the  $\beta$  protons have been assigned). Other unassigned resonances are mainly from the ends of long side chains. The presence of the heme group created both opportunities (some resonances were well separated, presumably due to their location near the heme) and obstacles (some resonance were difficult to find since they did not fall in the normal chemical-shift range). The discussion will focus on preliminary analysis of the data emphasizing elements of secondary structure and global fold. A short discussion of the assignments of the Met 61 side chain is included. During the final part of the preparation of this manuscript we became aware of another effort to assign the proton spectrum of cytochrome  $c_{551}$  from *P. aeruginosa* under different conditions. This will be discussed in an additional section.

**Secondary Structure Elements.** On the basis of the observation of long stretches of  $d_{NN}$  ( $i, i+1$ ),  $d_{\alpha N}$  ( $i, i+3$ ), and  $d_{\alpha N}$  ( $i, i+4$ ) connectivities, strong evidence for two helical regions could be found. These reach from Pro 3 to Asn 9 and from



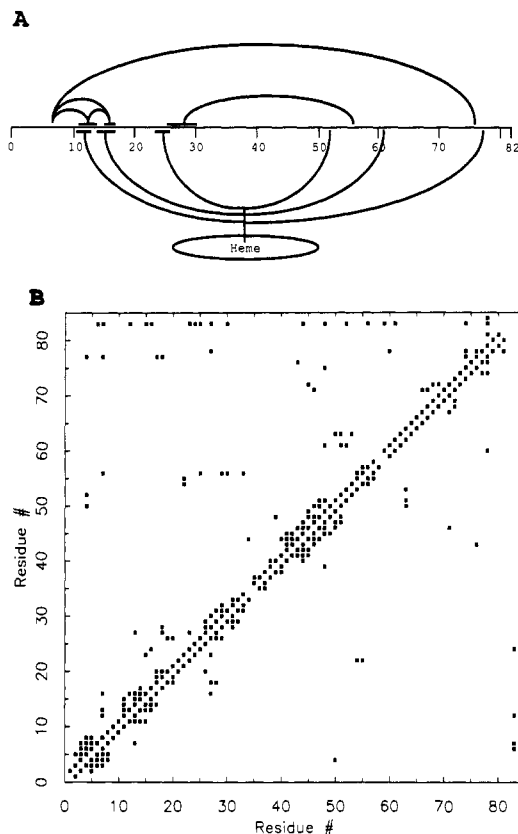


FIGURE 11: (A) Schematic representation of iron(II)  $c_{551}$  showing long-range NOEs within the polypeptide (above sequence) and from the peptide to the heme (below the sequence). Arcs from horizontal lines above and below the sequence show NOE contacts of several amino acids in that region. (B) Diagonal plot of interresidue NOEs observed in 150-ms 15 °C NOESY. The axes are the amino acid sequence numbers, with the 83rd residue being the heme group. Points in the upper left-hand triangle of the diagram are all NOE constraints, while those in the lower triangle are backbone-backbone constraints only.

Ala 40 to Ile 48 (Figure 10). This is in agreement with the X-ray crystal structure, which has four stretches of  $\alpha$ -helix from Pro 3 to Asn 9, Try 27 to Lys 33, Ala 40 to Lys 49, and Asp 68 to Ser 80 (Matsuura et al., 1982). The data of Figure 10 show that two other helical regions may be present around residue 30 and at the C-terminus. However, unambiguous identification of the crucial medium-range NOEs suffers from crosspeak overlap (Figure 10).

**Comparison to Crystal Structure.** Figure 11 is a schematic summary of the NOE crosspeaks observed and serves as a basis for comparison of the X-ray crystal (Matsuura et al., 1982) and solution structures of Fe(II)  $c_{551}$ . Figure 11A shows tertiary NOESY connectivities within the peptide and between the heme and peptide where arced lines indicate regions that are spatially close. Figure 11B is a diagonal plot showing interresidue NOE contacts. The Tyr 27 to Lys 33 helix is well constrained to the sequentially remote Trp 56 ring by the NOESY crosspeaks observed between backbone protons of Asp 29 and Val 30 to the Trp 56 ring. In addition, the Trp 56 2-proton gives a NOESY crosspeak with the  $\gamma$  meso proton of the heme, further constraining these regions of the peptide to one side of the heme. The  $H^{\alpha}$  proton of Glu 4 and the  $H^{\beta}$ s of Phe 7 show connectivities to the Trp 77 ring, indicating that portions of the C-terminal (Asp 68 to Ser 80) and N-terminal (Pro 3 to Asn 9) helices are in close proximity. Evidence for the turns near the N-terminus (Lys 8 to Gly 11 and Gly 11 to Ala 14) is shown in Figure 11A with NOESY crosspeaks between the Phe 7 (2,6) pair and the Cys 12  $H^{\beta}$ s, Phe 7 (3,5)

and Val 13  $H^{\alpha}$  and  $H^{\beta}$ s, and the Phe 7 4-proton with one of the His 16  $H^{\beta}$ s.

NOESY crosspeaks were observed from heme resonances ( $\alpha$  meso,  $\beta$  meso, and heme 3-methyl) to the peptide region Cys 12 to His 16. These NOEs are consistent with the heme and peptide being covalently attached via thioether linkages (Cys 12 and Cys 15) and axial metal ligation (His 16 to Fe). Connectivities were noted between the Pro 25  $H^{\beta}$  protons and the  $\gamma$  meso and between Val 23  $\gamma$ -CH<sub>3</sub>s and both the  $\gamma$  meso and heme 2-H proton, serving to constrain a nonhelical portion of the peptide to one side of the heme. Ile 48 showed strong NOESY connectivities to the  $\delta$  meso proton. Axial ligand Met 61 heme contacts are detailed in Figure 5B. Finally, Val 78  $\gamma$ -CH<sub>3</sub>s gave NOESY crosspeaks with the heme 8-methyl: this in addition to the previously mentioned Trp 77 2-proton heme contact constrains the C-terminus of the peptide to one side of the heme.

The chemical shifts of all but five of the  $\alpha$  protons are upfield of 4.7 ppm. This is consistent with the absence of a large content of  $\beta$ -sheet (Pardi et al., 1983). The 20 slowly exchanging amide protons are at locations where slow exchange would be expected according to the crystal structure ( $\alpha$ -helix). These observations, combined with the confirmation of the two longest helices in Fe(II)  $c_{551}$  (see above) and tertiary NOE data summarized in Figure 11 argue that the 2D  $^1H$  NMR data at pH = 6.8 are consistent with the X-ray crystal structure.

**Met 61 Side-Chain Assignments.** The axial Met 61 ligands had been previously assigned on the basis of NOE studies by Moore and co-workers (1977) ( $\epsilon$ -CH<sub>3</sub>-2.91 ppm;  $H^{\gamma}$  -3.53, -0.87 ppm;  $H^{\beta}$  -2.73, -0.51 ppm at 57 °C and pH = 7.0) and Senn and co-workers (1980) ( $\epsilon$ -CH<sub>3</sub> -2.90 ppm;  $H^{\gamma}$  -3.53, -0.51 ppm;  $H^{\beta}$  -2.73, -0.87 ppm at 52 °C and pH = 6.9), which have the assignments of one  $H^{\beta}$  and one  $H^{\gamma}$  exchanged. Our assignments are consistent with those of Senn et al. (1980) by showing scalar connectivity of both  $H^{\beta}$ s to the  $\alpha$  proton in the two-quantum spectrum.

**Comparison to Assignments at Different pH and Temperature.** The  $^1H$  resonances for Fe(II)  $c_{551}$  from *P. aeruginosa* have recently been obtained by another research group (Chau et al., 1990). Those assignments were obtained at pH = 3.5 at 60 °C, while our assignments were obtained at pH = 6.8 at 25 °C. A comparison of the chemical shift assignments showed that the majority of resonances were similar. However, there were several resonance assignments that are markedly different. In part, these differences can be explained with the differences in pH and temperature; in part, there are real discrepancies. The amide chemical shifts of Asp 2, Glu 4, and Ser 67 through Asp 69 differ by 0.36–0.71 ppm. These differences may be due to pH effects since these residues or the sequentially neighboring residues have carboxy groups at their side chains. However, the  $\alpha$ -proton chemical shifts of residues Pro 3, Pro 62, and Pro 63 differ by 0.5, 0.6, and 0.7 ppm, respectively. We found no evidence in our data that would be consistent with these assignments.

**Summary.** We have described the spin-system assignments for iron(II) cytochrome  $c_{551}$  from *P. aeruginosa* at pH = 6.8 (50 mM phosphate, 25 °C), including amino acids Glu 1 through Gln 81 (Lys 82 was not identified) as well as all heme resonances including the propionates. Sequential assignments in the proline-rich region (Pro 58 through Pro 63) were difficult; however, we are confident of the portions of those proline spin systems reported on the basis of sequential  $H^{\alpha}$  to  $H^{\beta}$  and amide to  $H^{\alpha}$  NOEs. The complete assignment of the axial iron ligand Met 61 was obtained through scalar connectivities.

Evidence was found at pH = 6.8 for two extended helical regions on the basis of medium-range NOEs ( $d_{\alpha(i),N(i+3)}$  and  $d_{\alpha(i),N(i+4)}$ ) along with slowly exchanging backbone amide protons marking the C- and N-termini, respectively. These data, in conjunction with other medium- and long-range NOEs to heme and peptide protons, are consistent with the overall fold as shown in the X-ray crystal structure.

## ACKNOWLEDGMENTS

We thank Dr. Marc Adler for help with a base-plane correction routine and with preparation of Figure 11B. We thank Dr. R. Timkovich for sending us a preprint of a manuscript on resonance assignments of cytochrome  $c_{551}$ .

## REFERENCES

- Ambler, R. P. (1963) *Biochem. J.* **89**, 341.
- Bax, A., & Davis, D. G. (1985) *J. Magn. Reson.* **65**, 355.
- Bechtold, R., Kuehn, C., Lepre, C., & Isied, S. (1986) *Nature (London)*, **322**, 286.
- Billeter, M., Braun, W., & Wüthrich, K. (1982) *J. Mol. Biol.* **155**, 321.
- Braunschweiler, L., & Ernst, R. R. (1983) *J. Magn. Reson.* **53**, 521.
- Chau, M.-H., Cai, M. L., & Timkovich, R. (1990) *Biochemistry* **29**, 5076.
- Farver, O., & Pecht, I. (1984) in *Copper Proteins and Copper Enzymes* (Lontie, R., Ed.) p 58, CRC, Boca Raton, FL.
- Farver, O., & Pecht, I. (1989) *Coord. Chem. Rev.* **94**, 17.
- Feng, Y., Roder, H., Englander, S. W., Wand, A. J., & Di Stefano, D. L. (1989) *Biochemistry* **28**, 195.
- Feng, Y., Roder, H., & Englander, S. W. (1990) *Biophys. J.* **57**, 15.
- Gray, H. B., & Malmström, B. G. (1989) *Biochemistry* **28**, 7499.
- Hoffman, B. M., & Ratner, M. A. (1987) *J. Am. Chem. Soc.* **109**, 6273.
- Horio, T. (1958) *J. Biochem. (Tokyo)* **45**, 195.
- Jeener, J., Meier, B. H., Bachmann, P., & Ernst, R. R. (1979) *J. Chem. Phys.* **71**, 4546.
- Keeler, J., Neuhaus, D., & Williamson, M. P. (1987) *J. Magn. Reson.* **73** (1), 46.
- Keller, R. M., & Wüthrich, K. (1978) *Biochem. Biophys. Res. Commun.* **83** (3), 1132.
- Keller, R. M., Wüthrich, K., & Pecht, I. (1976) *FEBS Lett.* **70** (1), 180.
- Kumar, A., Ernst, R. R., & Wüthrich, K. (1980) *Biochem. Biophys. Res. Commun.* **95**, 1.
- Leitch, F. L., Moore, B. R., & Pettigrew, G. W. (1984) *Biochemistry* **23**, 1831.
- Marcus, R. A., & Sutin, N. (1985) *Biochim. Biophys. Acta* **811**, 265.
- Marion, D., & Wüthrich, K. (1983) *Biochem. Biophys. Res. Commun.* **113**, 967.
- Matsuura, Y., Takano, T., & Dickerson, R. E. (1982) *J. Mol. Biol.* **156**, 389.
- McLendon, G., Pardue, K., & Bak, P. (1987) *J. Am. Chem. Soc.* **109**, 7450.
- Mitra, S., & Bersohn, R. (1982) *Proc. Natl. Acad. Sci. U.S.A.* **79**, 6807.
- Moore, G. R., Pitt, R. C., & Williams, R. J. P. (1977) *Eur. J. Biochem.* **77**, 53.
- Müller, L., & Ernst, R. R. (1979) *Mol. Phys.* **38**, 963.
- Pardi, A., Wagner, G., & Wüthrich, K. (1983) *Eur. J. Biochem.* **137**, 445.
- Parr, S. R., Barber, D., Greenwood, C., Phillips, B. W., & Melling, J. (1975) *Biochem. J.* **157**, 423.
- Piantini, U., Sørensen, O. W., & Ernst, R. R. (1982) *J. Am. Chem. Soc.* **104**, 6800.
- Rance, M., Sørensen, O. W., Bodenhausen, G., Wagner, G., Ernst, R. R., & Wüthrich, K. (1984) *Biochem. Biophys. Res. Commun.* **117**, 479.
- Richardson, J. S. (1981) *Adv. Protein Chem.* **34**, 166.
- Rosen, P., & Pecht, I. (1976) *Biochemistry* **15**, 775.
- Santos, H., & Turner, D. L. (1987) *FEBS Lett.*, **179**.
- Senn, H., Billeter, M., & Wüthrich, K. (1984) *Eur. Biophys. J.* **11**, 3.
- Senn, H., Keller, R. M., & Wüthrich, K. (1980) *Biochem. Biophys. Res. Commun.* **92** (4), 1362.
- Shaka, A. J., & Freeman, R. (1983) *J. Magn. Reson.* **51**, 169.
- Wagner, G., & Wüthrich, K. (1982) *J. Mol. Biol.* **155**, 347.
- Wagner, G., & Zuiderweg, E. R. P. (1983) *Biochem. Biophys. Res. Commun.* **113**, 854.
- Wagner, G., Kumar, A., & Wüthrich, K. (1981) *Eur. J. Biochem.* **114**, 375.
- Wagner, G., Neuhaus, D., Wörgötter, E., Vasak, V., Kägi, J. H. R., & Wüthrich, K. (1986) *Eur. J. Biochem.* **15**, 275.
- Wand, A. J., Di Stefano, D. L., Feng, Y., Roder, H., & Englander, S. W. (1989) *Biochemistry* **28**, 186.
- Wharton, D. C. (1978) *Methods Enzymol.* **53**, 646.
- Wilson, M. T., Greenwood, C., Brunori, M., & Antonini, E. (1975) *Biochem. J.* **145**, 449.
- Wüthrich, K., (1986) *NMR of Proteins and Nucleic Acids*, Wiley, New York.
- Wüthrich, K., & Wagner, G. (1978) *Trends Biochem. Sci.* **3**, 227.
- Wüthrich, K., Wider, G., Wagner, G., & Braun, W. (1982) *J. Mol. Biol.* **155**, 311.
- Yu, L. P., & Smith, G. M. (1990) *Biochemistry* **29**, 2914.